Journal of Fluorescence, Vol. 16, No. 3, May 2006 (© 2006)
DOI: 10.1007/s10895-005-0059-3

Laurdan in Fluid Bilayers: Position and Structural Sensitivity

Cíntia C. De Vequi-Suplicy,[1] Carlos R. Benatti,[1] and M. Teresa Lamy[1,2]

Received November 1, 2005; accepted December 23, 2005
Published online: May 9, 2006

Laurdan (2-dimethylamino-6-lauroylnaphthalene) is a hydrophobic fluorescent probe widely used in lipid systems. This probe was shown to be highly sensitive to lipid phases, and this sensitivity related to the probe microenvironment polarity and viscosity. In the present study, Laurdan was incorporated in 1,2-dipalmitoyl-*sn*-glycero-3-[phospho-*rac*-(1-glycerol)] (DPPG), which has a phase transition around 41°C, and DLPC (1,2-dilauroyl-*sn*-glycero-3-phosphocholine), which is in the fluid phase at all temperatures studied. The temperature dependence of Laurdan fluorescent emission was analyzed via the decomposition into two gaussian bands, a short- and a long-wavelength band, corresponding to a non-relaxed and a water-relaxed excited state, respectively. As expected, Laurdan fluorescence is highly sensitive to DPPG gel–fluid transition. However, it is shown that Laurdan fluorescence, in DLPC, is also dependent on the temperature, though the bilayer phase does not change. This is in contrast to the rather similar fluorescent emission obtained for the analogous hydrophilic probe, Prodan (2-dimethylamino-6-propionylnaphthalene), when free in aqueous solution, over the same range of temperature. Therefore, Laurdan fluorescence seems to be highly dependent on the lipid bilayer packing, even for fluid membranes. This is supported by Laurdan fluorescence anisotropy and spin labels incorporated at different positions in the fluid lipid bilayer of DLPC. The latter were used both as structural probes for bilayer packing, and as Laurdan fluorescence quenchers. The results confirm the high sensitivity of Laurdan fluorescence emission to membrane packing, and indicate a rather shallow position for Laurdan in the membrane.

KEY WORDS: Laurdan; fluorescence; lipid bilayers; fluid phase; bilayer packing; polarity; bilayer position.

INTRODUCTION

Prodan (2-dimethylamino-6-propionylnaphthalene) and its derivatives were introduced as solvent-sensitive probes by Weber and Farris [1]. They were designed with a donor and an acceptor group substituted opposite to a naphthalene ring, allowing the appearance of a large electric dipole, when excited, taking into consideration that the sensitivity of the fluorescent probe to the polarity of the environment is related to the magnitude of the excited state dipole moment. Among Prodan derivatives, Laurdan (2-dimethylamino-6-lauroylnaphthalene) has been widely used as a membrane probe, since it anchors in the bilayer due to its 12-carbon aliphatic tail, with the fluorescent moiety localized close to the bilayer surface (Fig. 1).

Laurdan fluorescence has been extensively used to characterize the gel–fluid phase transition in phospholipid membranes, and to identify phase coexistence in a large number of artificial and natural membranes [2–6]. In view of the great sensitivity of Laurdan to environment polarity [7–11], its fluorescent properties in membranes have been largely discussed in terms of the presence of water molecules at the different bilayer phases, at the fluorophore location, and their interaction with the excited state dipole. It is also known that the rate of solvent relaxation depends on the temperature and viscosity of the solvent [12]. Namely, when the molecular dynamics of solvent dipoles occur on the time scale of the probe

[1] Instituto de Física, Universidade de S. Paulo, CP 66318, CEP 05315-970, Sao Paulo, SP Brazil.
[2] To whom correspondence should be addressed. E-mail: mtlamy@if.usp.br

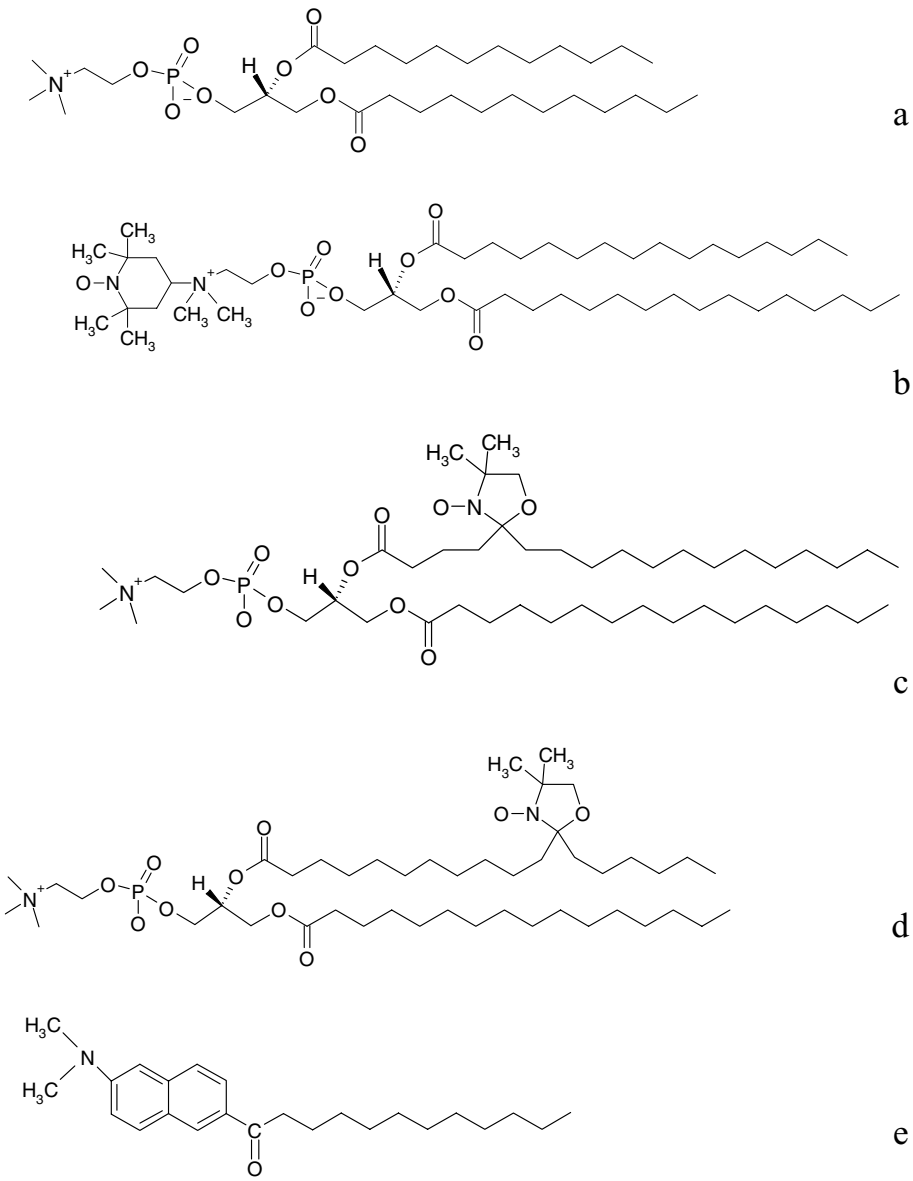

Fig. 1. Molecular structures: (a) DLPC, (b) Tempo-PCSL, (c) 5-PCSL, (d) 12-PCSL, (e) Laurdan.

fluorescence lifetime, a reorientation of solvent dipoles around the probe excited state may occur.

The presence of three different emitting populations has been proposed for Laurdan [13]. One related to the radiative deexcitation of a "locally excited" (LE) state, only present in apolar oils and frozen polar solvents (ethanol at -190°C). Due to a fast excited state reaction, attributed to an intramolecular rearrangement of the probe, in most solvents, or at a bilayer surface, two major excited states would be present, giving rise to two fluorescent bands, corresponding to the fluorescence of the solvent-relaxed and the solvent-non-relaxed charge transfer states (CTr and CT), respectively. Hence, both intramolecular and solvent relaxation processes would be responsible for the large Stokes shift displayed by this probe in polar solvents.

In lipid membranes, the maximum of the Laurdan emission fluorescent band displays a red shift of about 50 nm, when the bilayer goes from the gel to the fluid phase, as temperature increases [7]. This shift has been analyzed using a two excited state model, with the predominance of a short-wavelength band for the gel phase,

as compared to a long-wavelength emission for the fluid phase, related to radiative emissions from a non-relaxed and a solvent relaxed excited states, respectively.

The present work focus on Laurdan fluorescent properties in the fluid phase of 1,2-dilauroyl-*sn*-glycero-3-phosphocholine (DLPC), as compared to 1,2-dipalmitoyl-*sn*-glycero-3-[phospho-*rac*-(1-glycerol)] (DPPG), the latter presenting a gel–fluid transition around 41°C [14]. The emission spectra are analyzed as a composition of two gaussian bands, related to the emission of the two excited state populations, allowing a very precise evaluation of the relative presence of each population. Fluorescence anisotropy and spin labels are used to structurally characterize the site where the fluorescence moiety of Laurdan is localized.

MATERIALS AND METHODS

Materials

DLPC, DPPG, and 1,2-dioleoyl-*sn*-glycero-3-phosphocholine (DOPC) were purchased from Avanti Polar Lipids Inc. (Birmingham, AL). The fluorescent probes Laurdan (2-dimethylamino-6-lauroylnaphthalene) and Prodan (2-dimethylamino-6-propionylnaphthalene) are from Molecular Probes Inc. (Eugene, OR). The buffer Hepes (4-(2-hydroxyethyl) piperazine-1-ethanesulfonic acid) and EDTA (ethylenediaminetetraacetic acid) were purchased from Sigma Chemical Co. Milli-Q Plus water (Millipore) pH ~ 6 was used for buffer preparation. The spin labels, Tempo-PCSL (1,2-dipalmitoyl-*sn*-glycero-3-phospho(TEMPO)choline), 1-palmitoyl-2-stearoyl(5-DOXYL)-*sn*-glycero-3-phosphocholine (5-PCSL), and 1-palmitoyl-2-stearoyl(12-DOXYL)-*sn*-glycero-3-phosp -hocholine (12-PCSL) were purchased from Avanti Polar Lipids Inc. (Birmingham, AL).

Sample Preparation

For the steady-state fluorescent measurements, solutions of Laurdan and DLPC or DPPG in chloroform were prepared, to a final lipid concentration of 1 mM and Laurdan concentration of 1 μM. For ESR measurements, stock solutions of spin labels were prepared with DLPC and DOPC in chloroform to a final lipid concentrations of 10 mM and spin label concentration of 0.06 mM. With Prodan, a concentration of 1.13 μM was used in buffer. For the quenching measurements, a concentration of 0.05 mM of the quencher (5 mol% of the lipid concentration) was added to the lipid/Laurdan solution in chloroform. For all the samples, chloroform was evaporated under a stream of pure N_2 and the lipid/probe film was dried under low pressure for 2 h. The lipid/probe dry films were hydrated with 10 mM Hepes with 1 mM EDTA, pH 7.4, above the lipid phase transition temperature. The spectra were always measured immediately after sample preparation.

Fluorescence Measurement

Samples were placed in quartz cuvettes with optical pathways of 2 mm. The fluorescence emission and anisotropy were measured with a Fluorolog 3 Jobin YvonSPEX, model FL3-11, equipped with a xenon lamp, using 1.5 nm slits. The temperature was controlled with a thermal bath model Julabo HP 25, and was directly measured in the sample by a digital thermometer. The emission spectra were obtained with the excitation wavelength at 340 nm. The emission spectra of Laurdan were separated into two gaussian bands using the software *Origin 6.1*.

ESR Measurement

ESR measurements were performed with a Bruker EMX spectrometer. Field modulation amplitude of 1.0 G and microwave power of 10.13 mW were used. The temperature was controlled to about 0.2°C with a Bruker BVT-2000 variable temperature device. The temperature was monitored with a Fluke 51 K/J thermometer with the probe placed just above the cavity. The magnetic field was measured with a Bruker ER 035 NMR Gaussmeter, and, when necessary, the *WINEPR* software (Bruker) was used.

For the highly anisotropic spectra yielded by 5-PCSL, the order parameter and the isotropic hyperfine splitting (a_0) were calculated from the expressions [15, 16].

$$S_{\text{eff}} = \frac{A_{//} - A_{\perp}}{A_{zz} - \frac{1}{2}(A_{xx} + A_{yy})} \frac{a_{0c}}{a_0}, \quad a_0 = \frac{A_{//} + 2A_{\perp}}{3},$$

$$a_{0c} = \frac{A_{xx} + A_{yy} + A_{zz}}{3}$$

$$A_{//} \approx A_{\max}, \quad A_{\perp} = A_{\min}$$

$$+1.4 \left(1 - \frac{A_{\max} - A_{\min}}{A_{zz} - \frac{1}{2}(A_{xx} + A_{yy})}\right)$$

where $A_{\max}$ and $A_{\min}$ are the maximum and inner hyperfine splitting, respectively, directly measured in the ESR spectrum (see Fig. 7), and $A_{xx} = 5.9$ G, $A_{yy} = 5.4$ G, and $A_{zz} = 32.9$ G are the principal values of the hyperfine tensor for doxylpropane [17].

RESULTS AND DISCUSSION

Laurdan Fluorescence

Laurdan fluorescent emission spectra, at different temperatures, in DPPG and DLPC, are shown in Fig. 2a and b, respectively. A shift in the emission spectra for temperatures higher than 40°C can be clearly seen in Fig. 2a, in accord with the gel–fluid phase transition of DPPG, which is about 41°C. As expected, Laurdan in a gel bilayer emits around 440 nm, whereas in a fluid membrane the emission maximum shifts to 490 nm. As mentioned, this red shift has been attributed to an increase in the number/mobility of water molecules around Laurdan in the fluid phase, as compared to the gel phase, therefore increasing the probe/solvent dipolar relaxation [7].

However, a not so drastic but similar shift on the Laurdan emission band can be observed when the fluorophore is incorporated in DLPC bilayer (Fig. 2b), though the membrane is in the fluid state at the whole range of temperatures studied.

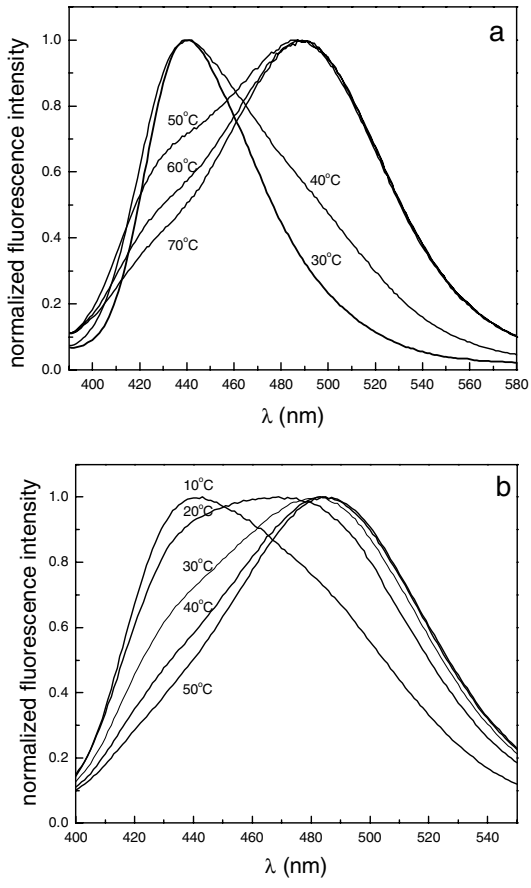

Fig. 2. Fluorescence emission spectra of Laurdan in (a) DPPG and (b) DLPC at different temperatures.

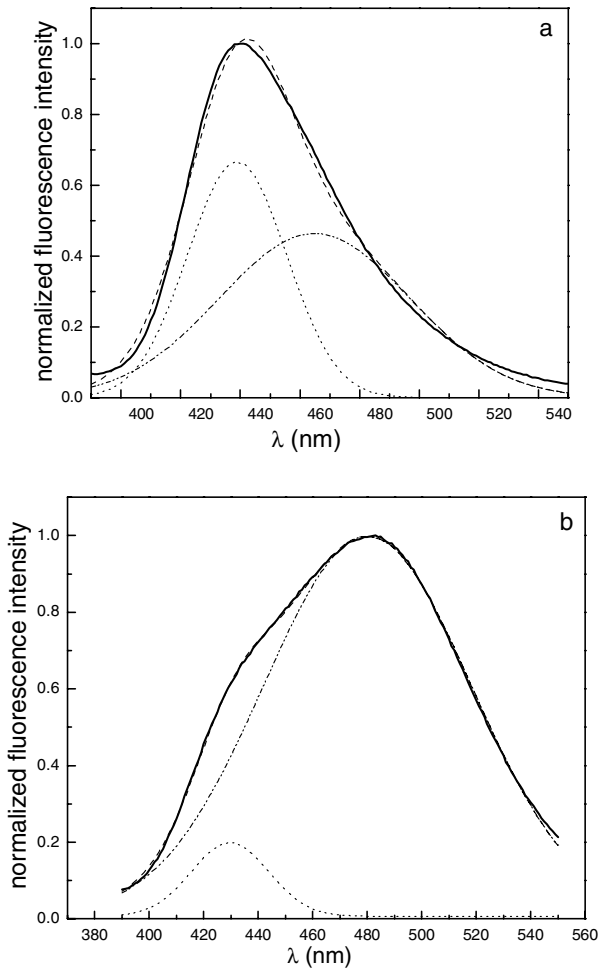

Fig. 3. Decomposition of the fluorescence emission spectra of Laurdan in (a) DPPG and (b) DLPC, in buffer, at 30°C: full line (—) is the experimental spectrum; dot (. . .) and dash-dot lines (–·–) are the short-wavelength and long-wavelength gaussian bands, respectively; dash line (– –) is the sum of the two gaussians.

The Laurdan fluorescent emission spectra, at all temperatures studied, in both DPPG and DLPC, can be well analyzed as a composition of two gaussian lines, centered around 430 and 480 nm, as shown in Fig. 3a and b. Therefore, confirming that the fluorescence decay is mainly due to transitions from two different excited energy levels only. The fraction of the areas of the two gaussians used in the fittings is shown in Fig. 4, for Laurdan in the two lipid bilayers, as a function of temperature. The analysis of the spectra through the decomposition into two bands allows a clear evaluation of the percentage of each emitting population. Hence, for that purpose, it is a better analysis than the generalized polarization [7], GP, which measures a normalized intensity relationship $((I_{440}-I_{490})/(I_{440}+I_{490}))$. GP does not completely separate the

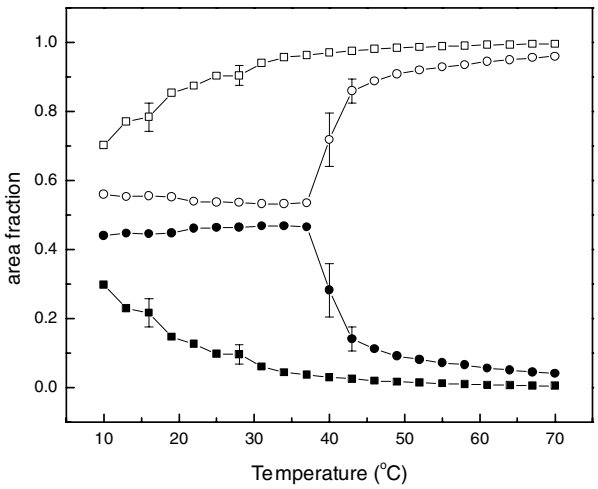

Fig. 4. Temperature variation of the fraction of the areas of the two gaussian components that give the best fit of the Laurdan fluorescence spectra in (○, ●) DPPG and (■, □) DLPC. Open and full symbols used for long- and short-wavelength bands, respectively. The data are mean values of three different samples, and the uncertainties are the standard deviations, not shown if they are smaller than the size of the symbols.

contributions of the two excited states. Though the fluorescence emission at 490 nm is almost only due to the relaxed excited state, at 440 nm both bands are present (see Fig. 3).

The DPPG gel–fluid transition can be very well monitored by the relative area of the two bands: there is a sharp drop on the short-wavelength band area, naturally parallel to a sharp increase on the long-wavelength band. Surprisingly, the two bands are nearly equally present in DPPG gel phase, their relative areas presenting almost no dependence on temperature, showing that even in the gel phase half of the emission energy comes from the relaxed excited state.

When inserted in a fluid bilayer, either in DPPG or DLPC, Laurdan fluorescent decay is mainly due to the long-wavelength transition, therefore to the relaxed excited state (Fig. 4). It is important to point out that for the fluid phase of DLPC, from 10 to 40°C, there is a significant increase in the population emitting from the relaxed excited state. Above 40°C, almost all the Laurdan fluorescent emission is due to the low energy excited state only.

For both lipids, the center of the gaussians for the best fittings presented a small variation with temperature. As temperature increases, from 10 to 70°C, the position of the short-wavelength band presents a continuous blue shift, whereas the position of the long-wavelength peak shifts to the red side (Table I). This is an interesting experimental result, needing more investigation. Though a theoretical approach is out of the scope of the present

Table I. Peak Positions of the Two Gaussian Curves, and Errors (χ^2), Found for the Best Fittings of Laurdan Fluorescence Spectra in DPPG and DLPC, at Various Temperatures

	Short-wavelength peak (nm)		Long-wavelength peak (nm)		χ^2	
T (°C)	DPPG	DLPC	DPPG	DLPC	DPPG	DLPC
10	437.4	435.4	462.8	473.4	0.996	0.995
13	437.5	435.4	463.2	475.2	0.996	0.994
16	437.6	434.8	463.2	475.2	0.996	0.995
19	437.6	434.8	463.6	478.3	0.996	0.996
22	438.7	433.7	466.2	477.5	0.996	0.996
25	438.6	432.8	466.6	478.3	0.996	0.997
28	437.8	432.6	465.3	480.1	0.996	0.998
31	437.9	430.8	466.3	479.8	0.996	0.998
34	438.9	430.3	469.5	482.2	0.962	0.999
37	438.1	428.8	469.3	481.2	0.995	0.999
40	435.7	427.8	477.9	482.0	0.995	0.999
43	430.6	426.7	481.2	482.5	0.997	0.999
46	429.0	425.4	482.5	483.0	0.998	0.999
49	427.8	424.8	483.7	483.2	0.999	0.999
52	426.9	423.3	484.3	483.8	0.999	0.998
55	426.2	422.7	485.1	483.9	0.999	0.998
58	425.3	421.4	485.6	484.3	0.999	0.998
61	424.6	420.0	486.0	484.5	0.999	0.998
64	423.9	418.9	486.3	484.8	0.999	0.998
67	423.2	417.3	486.4	485.9	0.999	0.998
70	422.5	416.2	486.5	484.6	0.999	0.998

Note. The wavelength data are mean-values of three different samples, with less than 0.5% deviations.

work, one could speculate that the shift to longer wavelengths, as temperature increases, hence a decrease in the average emission energy, is due to the predominance of transitions from more relaxed excited sub-states due to the molecule and/or solvent movement. The blue shift detected for the so-called non-relaxed charge transfer excited state, as temperature increases, needs a more complex rationalization.

Interestingly, the difference in the population of the two Laurdan excited states in fluid DLPC does not seem to be related to the temperature variation only, as the fluorescent emission of the analogous hydrophilic probe Prodan in water solution is insensitive to temperature variation, from 10 to 50°C (Fig. 5). Hence, the balance between the two Laurdan excited populations is dependent on the packing of the fluid DLPC bilayer, which is sensitive to the temperature. And the packing of the membrane defines the rigidity of the water molecules at the bilayer surface, around the fluorophore.

To analyze the bilayer packing at the Laurdan position, Laurdan fluorescence anisotropy was measured (Fig. 6). As expected, Laurdan anisotropy can well monitor the DPPG phase transition, as shown in Fig. 6a.

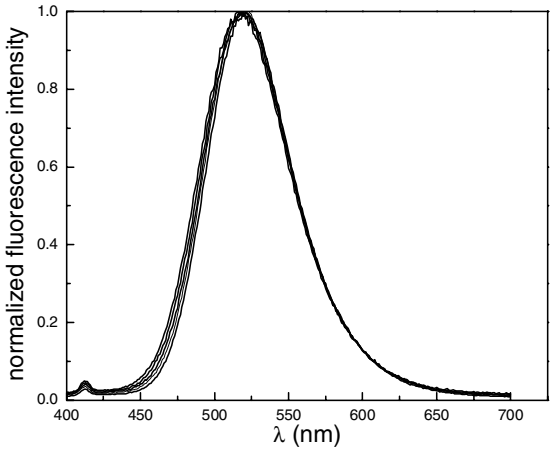

Fig. 5. Emission spectra of 1.13 μM Prodan in buffer solution, at 10°C, 20°C, 30°C, 40°C, and 50°C.

Curiously, the fluorescence anisotropy measured at the short-and long-wavelength positions yielded rather different values, mainly for the fluid phases of DPPG and DLPC. The anisotropy measured at the long-wavelength position, 480 nm, is much lower than that measured at the short-wavelength position, 430 nm. That could possibly be due to a shorter lifetime for the non-relaxed excited state [18], allowing a shorter time for the excited fluorophore rotational diffusion, resulting in a higher anisotropy value. Alternatively, one could think about the coexistence of two different average positions for the Laurdan fluorophore in the bilayer: one at the water/lipid interface, rather mobile, mainly decaying at 480 nm; and the other one less mobile, inside the bilayer, hence less water relaxed, decaying at a shorter wavelength, 430 nm. Time-resolved fluorescence would be important for that discussion.

In the gel phase of DPPG, the Laurdan anisotropy is nearly temperature independent, indicating that the bilayer packing does not change from 10 to 38°C. That can be correlated to the invariance in the equilibrium of the two excited populations over the same range of temperature (Fig. 4).

In the fluid phase of DLPC (Fig. 6b), the temperature variation of the Laurdan anisotropy clearly indicates that the bilayer microenvironment where the fluorophore is inserted is becoming looser as the temperature increases. That is certainly related to the increase in the relaxed excited state population with temperature (Fig. 4). Above 40°C, the bilayer packing keeps getting looser, as indicated by the decrease in Laurdan fluorescence anisotropy, but the probe/solvent dipolar relaxation process is complete, as the equilibrium between the two

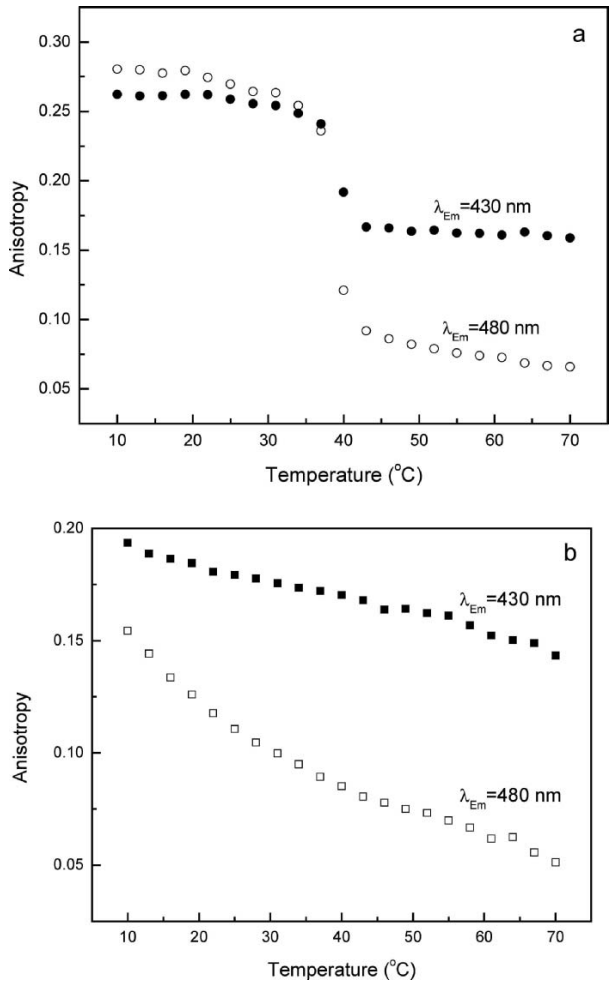

Fig. 6. Laurdan fluorescence anisotropy in (a) DPPG and (b) DLPC, at two different emission wavelengths, 430 and 480 nm, corresponding to the short (full symbols) and long (open symbols) wavelength bands. The data are mean values of three different samples. All the calculated standard deviations were found to be smaller than the size of the symbols.

emitting populations is temperature independent (Fig. 4). However, the Laurdan fluorescence spectrum is rather different from that of Prodan in aqueous medium (Fig. 5), possibly indicating that the number and/or dynamics of water molecules surrounding Laurdan at the bilayer surface are different from those in bulk water.

Spin Labels as Structural Probes

Spin labels have been extensively used to monitor the viscosity and polarity of microenvironments in lipid membranes [see, for instance, 19–22]. In order to further analyze the dependence of the packing and polarity of DLPC bilayers with temperature, two different spin labels were used close to the membrane surface, where

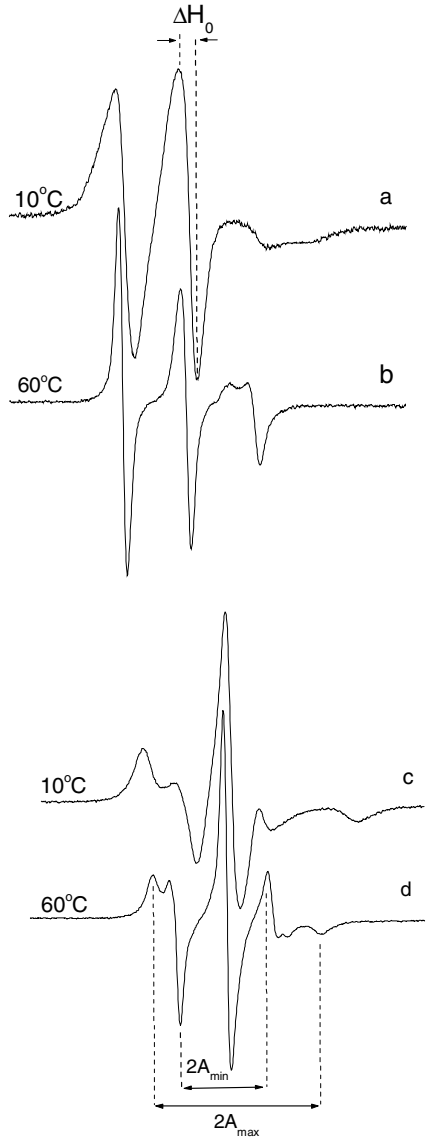

Fig. 7. ESR spectra of Tempo-PCSL in DLPC at (a) 10°C and (b) 60°C, and 5-PCSL in DLPC at (c) 10°C and at (d) 60°C.

the fluorescent moiety of Laurdan is suppose to reside [8]: Tempo-PCSL and 5-PCSL (Fig. 1), which monitor, respectively, the membrane interface and the bilayer position close to the fifth acyl carbon atom. To get a better insight in to the variation of the packing of fluid bilayers with temperature, the same spin labels were also incorporated in the fluid bilayer of DOPC, which has the same polar headgroup as DLPC, but two chains with 18 carbon atoms with one insaturation each, being in the fluid phase for temperatures above zero.

The spectra of Tempo-PCSL and 5-PCSL incorporated in the bilayers, at 10 and 60°C, are rather different

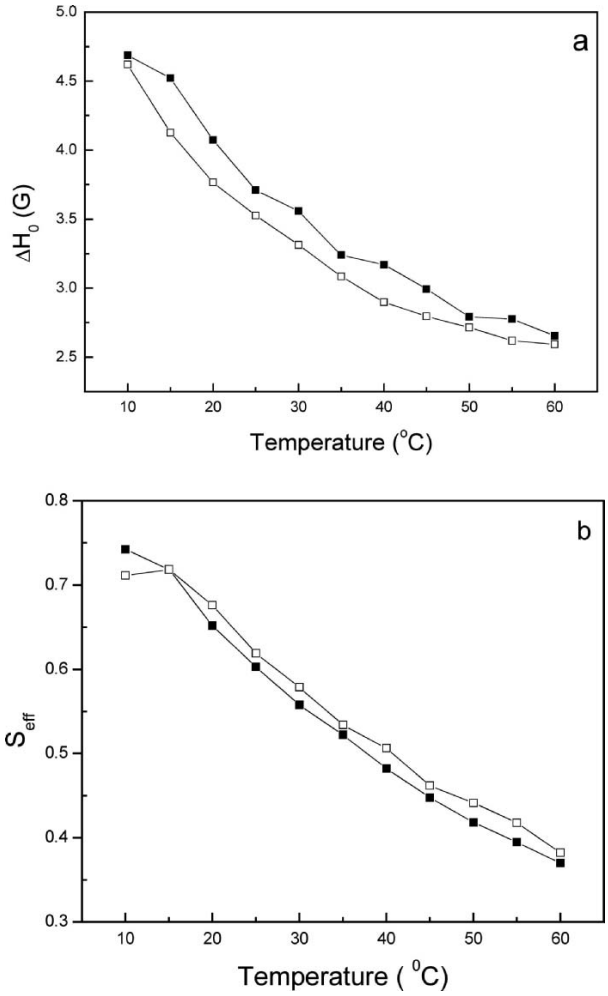

Fig. 8. Temperature dependence of the (a) central line line width (ΔH_0) measured on the ESR spectra of Tempo-PCSL and (b) effective order parameter (S_{eff}) of 5-PCSL in (■) DLPC and (□) DOPC.

(Fig. 7), evidencing the variation in the bilayer packing with temperature, and the great structural sensitivity of spin labels. Moreover, the much more anisotropic spectra of 5-PCSL, as compared to those of Tempo-PCSL, evidences the greater packing and order around the fifth chain carbon atom, as compared to the bilayer surface [17].

For the Tempo-PCSL the best experimental parameter to be used over the whole range of temperature, sensitive to bilayer packing, is the central line width (ΔH_0 shown in Fig. 8). Interestingly, the two fluid bilayers, DLPC and DOPC, show very similar mobility at the bilayer interface (Fig. 8a). Around the fifth carbon atom, 5-PCSL also indicates that the two lipids present very similar packing. The parameter used to analyze the 5-PCSL spectra was the effective order parameter, S_{eff} (see Materials and methods section), which contains

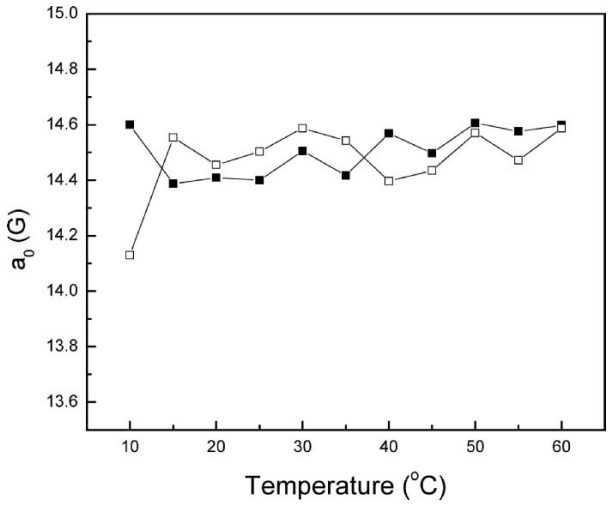

Fig. 9. Temperature dependence of the isotropic hyperfine splitting a_0, measured on the ESR spectra of 5-PCSL in (■) DLPC and (□) DOPC.

contributions from both order and rate of motion, although the principal contribution to S_{eff} is the amplitude of segmental motion of the acyl chains [23]. Hence, though both DLPC and DOPC are in the fluid phase at all temperatures studied, the packing of the bilayer surface varies considerably with temperature. These results with spin labels are in accordance with those yielded by Laurdan fluorescence anisotropy (Fig. 6).

Considering that the variation on the Laurdan fluorescent emission spectra has been also discussed based on the variation of the number of water molecules around the fluorophore, the ESR spectra of the spin labels incorporated in the bilayers were analyzed for possible nitroxide microenvironment polarity changes. It has been shown that the magnitude of the nitrogen isotropic hyperfine splitting (a_0, one-third of the trace of the hyperfine tensor) depends on several factors, which increases the unpaired electron spin density at the nitrogen nucleus, [24]. For labels inside a lipid bilayer, there are strong indications that an increase in a_0 is mainly related to the increase in the amount of nitroxide–water hydrogen bonding. Therefore, the presence of water in the bilayer can be estimated from the magnitude of the isotropic nitrogen hyperfine splitting. The nitrogen isotropic hyperfine splitting a_0 can be relatively well determined in ESR spectra typical of probes displaying high order and fast movement, where the A_{max} and A_{min} values can be precisely measured (see Materials and methods section) like those of 5-PCSL (Fig. 7d). Figure 9 shows that the polarity around the fifth carbon atom is nearly invariant with temperature, for the two lipids in the fluid phase. Though this is interesting for bilayers structural characterization, it is not conclusive for discussing Laurdan sensitivity to water molecules, as will be shown in the next section. Unfortunately, the ESR spectra of Tempo-PCSL do not allow an obvious measurement of the isotropic hyperfine splitting.

Spin Labels as Laurdan Fluorescence Quenchers

For a better understanding of the Laurdan position in fluid bilayers, spin labels with the paramagnetic center bound at different acyl carbon atoms (Tempo-PCSL, 5-, and 12-PCSL) were used as quenchers of the Laurdan fluorescence in DLPC bilayers, at different temperatures (Fig. 1). Figure 10 shows, comparatively, the fluorescence emission of Laurdan incorporated in DLPC bilayer, in the absence and in the presence of the quenchers. Interestingly, the Laurdan fluorescence suppression by nitroxides at the 5th and 12th carbon atoms is rather similar. That is possibly due to the mobility of the hydrocarbon chain in a 12-carbon atoms bilayer as DLPC, making the N–O group at both positions almost equally accessible to the fluorophore. However, Tempo-PCSL is clearly more effective in suppressing Laurdan fluorescence, indicating that the fluorophore is localized at the bilayer surface, closer to the position where the paramagnetic moiety of Tempo-PCSL resides. Also interesting is the observation that Tempo-PCSL clearly quenches the emission of the more relaxed (long wavelength) state preferentially. Again, that could be related to a longer lifetime for the Laurdan water-relaxed excited state, but, for further discussion, a comprehensive study of Laurdan fluorescence suppression, with static and time-resolved fluorescence would be necessary.

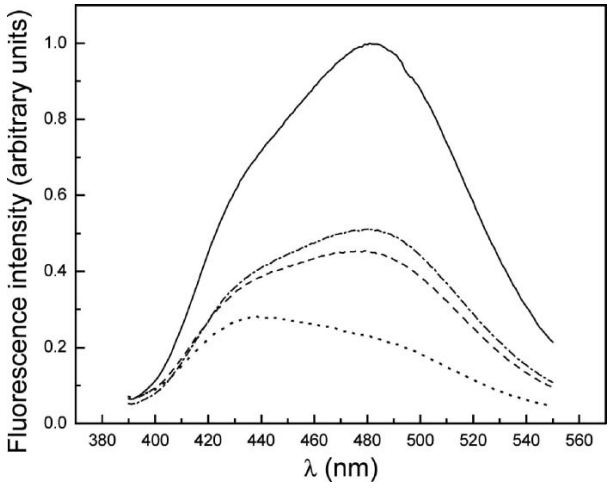

Fig. 10. Fluorescence emission spectra of Laurdan (—) in pure DLPC, and in DLPC with the quenchers (. . .) Tempo-PCSL, (–·–) 5-PCSL, and (—-) 12-PCSL at 30°C.

CONCLUSIONS

Laurdan fluorescence, both in DPPG and DLPC, can be well decomposed into two gaussian bands. This decomposition allows a clear evaluation of the balance between the two emitting populations: a non-relaxed and a water-relaxed. In fluid DLPC bilayers, the equilibrium between the two excited states is dependent on the bilayer surface packing, up to 40°C. For higher temperatures, though the bilayer surface structure keeps changing, as monitored by Laurdan fluorescence anisotropy, and spin labels, Laurdan fluorescence emission spectrum is insensitive to the changes. The sensitivity of Laurdan fluorescence to the increase in fluidity of DLPC bilayers, from 0 to 40°C, is possibly related to the increase in the mobility of the water molecules at the membrane surface. The faster movement of the molecules would facilitate their equilibrium around the Laurdan excited state dipole, increasing the population of the relaxed long-wavelength excited state. The great difference in the Laurdan fluorescence spectra when incorporated in gel and fluid membranes could be mainly due to the mobility of the water molecules around the fluorophore, and not to the amount of water molecules at the bilayer surface.

Laurdan fluorescence quenching by nitroxides strongly indicates that the fluorescence moiety of Laurdan is localized at the lipid bilayer surface closer to the position where the N–O group of Tempo-PCSL resides, as compared to the position of the fifth carbon atom, where the 5-PCSL paramagnetic group is localized.

Interestingly, for Laurdan in DPPG in the gel phase, half of its radiative deexcitation originates from the relaxed excited state. That indicates that even in this lipid packed phase, at the bilayer position where Laurdan resides, there is a considerable probability of water rearrangement around the excited state dipole.

ACKNOWLEDGMENTS

This work was supported by USP, FAPESP and CNPq. Fellowships for C.C.V.S. (FAPESP), C.R.B. (FAPESP) and M.T.L. (CNPq) are acknowledged.

REFERENCES

1. G. Weber and F. J. Farris (1979). Synthesis and spectral properties of hydrofobic fluorescent probe: 6-Propionyl-2-(dimethylamino)naphthlene. *Biochemistry* **18**, 3075–3078.
2. L. A. Bagatolli, E. Gratton, and G. D. Fidelio (1998). Water dynamics in glycosphingolipid aggregates studied by LAURDAN fluorescence, *Biophys. J.* **75**, 331–341.
3. D. Zubiri, A. Domecq and D. L. Bernik (1999). Phase behavior of phosphatidylglycerol bilayers as a function of buffer composition: Fluorescence studies using Laurdan probe, *Coll. Surf. B Biointer.* **13**, 13–28.
4. L. A. Bagatolli, T. Parasassi, G. D. Fidelio, and E. Gratton (1999). A model for the interaction of 6-Lauroyl-2-(*N*,*N*-dimethylamino)naphthalene with lipid environments: Implications for spectral properties, *Photochem. Photobiol.* **70**(4), 4.
5. L. A. Bagatolli and E. Gratton (1999). Two-photon fluorescence microscopy observation of shape changes at the phase transition in phospholipid giant unilamellar vesicles, *Biophys. J.* **77**, 2090–2101.
6. S. Vanounou, D. Pines, E. Pines, A. H. Parola and I. Fishov (2002). Coexistence of domains with distinct order and polarity in fluid bacterial membranes, *Photochem. Photobiol.* **76**(1), 1–11.
7. T. Parasassi, G. Stasio, G. Ravagnan, R. M. Rusch, and E. Gratton (1991). Quantization of lipids phases in phospholipid vesicles by the generalized polarization of Laurdan fluorescence, *Biophys. J.* **60**, 179–189.
8. T. Parasassi, E. K. Krasnowska, L. Bagatolli, and E. Gratton (1998). LAURDAN and PRODAN as polarity-sensitive fluorescent membrane probes, *J. Fluorescence* **8**, 365–373.
9. R. M. Epand and R. Kraayenhof (1999). Fluorescent probes used to monitor membranes interfacial polarity, *Chem. Phys. Lipids* **101**, 57–64.
10. R. B. Campbell, S. V. Balsubramanian, and R. M. Straubinger (2001). Phospholipd–cationic lipid interactions: Influences on membrane and vesicles properties, *Biochim. Biophys. Acta* **1512**, 27–39.
11. T. Söderlund, J. M. I. Alakoskela, A. L. Pakkanen, and P. K. J. Kinnunen (2003). Comparison of the effects of surface tension and osmotic pressure on the interfacial hydration of a fluid phospholipid bilayer, *Biophys. J.* **85**, 2333–2341.
12. J. R. Lakowicz (1999) *Principles of Fluorescence Spectroscopy*, 2nd ed. Kluwer Academic/Plenum Press, New York, pp. 185–289.
13. M. Viard, J. Gallay, M. Vincent, O. Meyer, B. Robert and M. Paternostre (1997). Laurdan solvatochromism: Solvent dielectric relaxation and intramolecular excited-state reaction, *Biophys. J.* **73**, 2221–2234.
14. D. Marsh (1990) *CRC Handbook of Lipids Bilayers*. CRC Press, Boca Raton, Florida, pp. 219.
15. O. H. Griffith and P. C. Jost (1976) Lipids spin labels in biological membranes. In: L. J. Berliner (Ed.), *Spin Labelling. Theory and Applications*. Academic Press, New York, p. 453.
16. B. J. Gaffney (1976) Practical considerations for the calculations of order parameters for fatty acid or phospholipid spin labels in membranes. In: L. J. Berliner (Ed.), *Spin Labelling. Theory and Applications*. Academic Press, New York, p. 567.
17. W. L. Hubbell, and H. M. McConnell (1971). Molecular motion in spin-labeled phospholipids and membranes, *J. Am. Chem. Soc.* **93**, 314–326.
18. M. Viard, J. Gallay, M. Vincent and M. Paternostre (2001). Origin of Laurdan sensitivity to the vesicle-to micelle transition of phospholipids–octylglucoside system: A time-resolved fluorescent study, *Biophys. J.* **80**, 347–359.
19. D. Marsh (1981). Electron spin resonance: Spin labels. In: E. Grell (Ed.), *Membrane Spectroscopy*. Springer, Berlin, pp. 51–142.
20. C. R. Benatti, E. Feitosa, R. M. Fernandez and M. T. Lamy-Freund (2001). Structural and thermal characterization of dioctadecyldimethylammonium bromide dispersions by spin labels, *Chem. Phys. Lipids* **111**, 93–104.
21. C. R. Benatti, J. M. Ruysschaert. and M. T. Lamy (2004). Structural characterization of diC_{14}-amidine, a pH sensitive lipid used for transfection, *Chem. Phys. Lipids* **131**, 197–204.
22. R. M. Fernadez and M. T. Lamy-Freund (2000). Correlation between the effects of a cationic peptide on the hydration and fluidity of anionic lipid bilayers: A comparative study with sodium ions and cholesterol, *Biophys. Chem.* **87**, 87–102.
23. H. Schindler and J. Seelig (1973). EPR-spectra of spin labels in lipid bilayers, *J. Chem. Phys.* **59**(4), 4.
24. O. H. Griffith, P. J. Dehlinger and S. P. Van (1974). Shape of hydrophobic barrier of phospholipid bilayers (evidence for water penetration in biological membranes), *J. Membrane Biol.* **15**, 159–192.